

Hyp Hyp Hooray

First version: 9th June 2007

This version: 4th January 2010

Abstract

A new stochastic-local volatility model is introduced. The new model's structural features are carefully selected to accommodate economic principles, financial markets' reality, mathematical consistency, and ease of numerical tractability when used for the pricing and hedging of exotic derivative contracts. Also, we present a generic analytical approximation for Black [Bla76] volatilities for plain vanilla options implied by any parametric-local-and-stochastic-volatility model, apply it to the new model, and demonstrate its accuracy.

1 Introduction

The use of stochastic volatility models has become popular in financial mathematics, both with practitioners and in academia. The reasons for the use of stochastic volatility models differ across researchers working on different underlying financial markets. For some, they are predominantly a mechanism to have control over the curvature of the model-implied volatility smile. For others, they are a representation of the actual uncertainty of asset class volatility, and used to model its impact on exotic derivatives that depend significantly on the variation of short term realised volatility such as volatility and variance swaptions, globally capped and/or floored cliquets, Napoleons, options on CPPIs, and so on. Whilst the use of these models is widespread, and the reasons for their use are diverse, the actual number of different models used in practice is comparatively small. A very popular one, the so-called SABR model [HKL02], appears to be used predominantly for the marking and management of implied volatility surfaces. Similarly, some stochastic volatility research is explicitly targeted at a better understanding of the impact stochastic volatility has on the probability distribution of the underlying financial asset class such as the excellent works by Fouque [FPS00] and Gatheral [Gat04, Gat06]. With respect to the consistent use of a stochastic volatility model for both vanilla options' smile representation and numerical evaluation of exotic derivatives, the most popular model at the time of this writing is almost certainly the Heston [Hes93] model, and possibly its extensions with Constant Elasticity of Variance [Lip02, AL05, For06] for local volatility (albeit that Lipton in his seminal article [Lip02] also discussed quadratic volatility). In comparison, researchers into the scaling of volatility of volatility as a function of the level of volatility suggest that the stochasticity of volatility observed in the market is probably closer to the SABR (also known as Scott [Sco87], Hull-White [HW88], and Wiggins [Wig87]) model [Wig87, Wil06]. In summary, it seems to emerge nowadays that the main reason the Heston model started being used is that there are analytics for its calibration, and not that it matches market dynamics particularly realistically. In terms of its numerical tractability, it turns out that the Heston model is not as *analytically* solvable as was first thought, nor that its numerical implementation by means of Monte Carlo simulations or finite difference solving is as trivial as one might hope [Klu02, AA02, MN03, KJ05, And07, AMST07].

*OTC Analytics

†Commerzbank Corporates & Markets

Whilst the SABR model seems to have a better representation of the scaling of volatility of volatility with the level of instantaneous volatility, it has its own drawbacks. For starters, the most commonly used vanilla option pricing approximation [HKL02] does not permit for term structures of parameters nor for mean reversion of volatility as it was proposed in the original formulations of the model [Sco87, HW88], albeit that some progress seems to have been made in the direction of remedying that [Osa06, HL05]. Alas, for a decent fit to market observable implied volatility smiles, term structures of risk-neutral parameters are often needed. Equally worrying, not having the process for volatility to mean-revert means that the uncertainty in *relative* volatility grows indefinitely over time, which is in contrast with both market implied levels and basic economics. Further, the SABR dynamics, unfortunately, have recently been found to give rise to serious concern as to whether second and higher moments of the underlying financial observable are well defined or not [AP04]. This last point is a rather subtle one with several implications. For one, it means that many analytical approximations for mildly volatility smile dependent products such as CMS swaps are not necessarily convergent, a feature that is somewhat reminiscent of the explosion of futures prices in instantaneously lognormal interest rate models [HW93, SS94]. Secondly, any *numerical* implementation is prone to suffering from suddenly arising convergence failures. This can happen both for finite differencing methods as well as for Monte Carlo simulations, and any practitioner who has been called over by a trader and had to explain why, for a certain product with associated market observable implied volatility smile, the respective simulation model every now and then shows a path that is a complete outlier knows what I am referring to. What all this amounts to is this: there is a need for a new stochastic volatility model that is designed to have the same desirable properties as all the above, but fewer, or ideally none, of the undesirable ones.

Since short term skews are very difficult to calibrate with purely stochastic volatility models, local volatility extensions have become popular. Also, in order to simplify issues arising from the volatility process on the chosen measure, some practitioners favour to use local volatility techniques to explain the *skew* of the implied volatility profile, and use the stochasticity of volatility to match the curvature [Pit03, Pit07]. Alas, the most commonly used local volatility extensions for which analytical approximations for plain vanilla options are known, namely the Constant Elasticity of Variance model [CR76] and the Displaced Diffusion model [Rub83] both have the feature that for some asset classes such as equities or commodities, when calibrated to the observable skew, allow for the underlying asset value to attain zero, or even cross over into the negative domain. For many contracts, as for instance common for interest derivatives, this is no issue. However, many other derivative contracts involve the concept of *forward performance* whereby the ratio of two future fixings at times T_1 and T_2 is used as the effective underlying for a final payoff. These financial products have no well defined expected value when the underlying can attain zero. Even when the case of the underlying value dropping to zero is handled by an explicit rule in the derivatives payoff description, it is economically undesirable to have significant contributions from the positive probability of being at zero or below, as is usually the case for market-calibrated CEV or displaced diffusion local volatility models. In a nutshell, just like there is a need for a different stochastic volatility setting, there is also some advantage to be gained from revisiting the question as to what local volatility model make sense.

The work presented in this article is twofold: first, we introduce a new type of stochastic volatility model that is carefully designed to be as close as possible in its parametric notation to the SABR and CEV family of models for the sake of easing any user's transition, yet different in all aspects where existing models cause difficulty. The second part consists of analytical approximations for vanilla options. Good analytical approximations help the handling of a model in two ways: on the one hand, they accelerate calibration to market-observable volatility surfaces, and on the other hand, they help in our understanding of the model's analytical features. This latter point is not to be underestimated since the way a new model responds to moves of the parameters or underlying quantities is a crucial criterion for its application in a trading environment.

In this article, we employ perturbative expansion techniques to arrive at analytical expressions for vanilla option prices and implied Black volatilities. Techniques of this kind tend to start with a scaling assessment, and the choice of a parameter that is, at least initially, assumed to be small, albeit that this requirement is typically dropped in a final stage of the expansion. The choice of smallness parameter determines the nature and applicability of the expansion results. For instance, Fouque et. al. [FPS00] have derived some important results based on the assumption of fast mean reversion of volatility, essentially making the reciprocal of the mean reversion parameter their smallness quantity. Whilst their published expansions are of low order, some very useful lessons such as the scaling of skew with correlation between volatility and underlying can be learned from their analysis. The work of Rasmussen and Wilmott [RW03] is based on an expansion in the ratio of volatility of volatility to mean reversion strength, which is very similar in spirit to the work of Fouque et. al. Crucially, both [FPS00] and [RW03] choose a setting in which the uncertainty of volatility is bounded, i.e. it is assumed that, over time, the distribution of volatility converges to a stationary state. It is this feature that makes both their work akin to what is known as *ergodic* expansions in theoretical physics and statistical mechanics, which is a term that stands for the replacement of time averages with spatial averages, i.e. a replacement of temporal averages with averages over the stationary distribution, specifically of volatility in this context. The main difference between [FPS00] and [RW03] is that Fouquet et. al. start off with volatility given by a smooth function of a standard Ornstein-Uhlenbeck process, whereas Rasmussen and Wilmott begin with an explicit stochastic differential equation for volatility. Whilst the two approaches are in principle equivalent, the difference in sheer algebraic complexity makes it prohibitively difficult to move to higher order expansions in the setup of [FPS00]. Using an ingenious set of analytical transformations based on ordering by the relative noise-strength-to-reversion-speed-ratio, in a set of hierarchical equations not dissimilar to *multiple time scaling expansions*, Rasmussen and Wilmott, instead, arrive at asymptotic expressions of significantly higher order. Both Fouque et. al.'s and Rasmussen and Wilmott's works are most applicable for moderate to large times to expiry, and, alas, do not include the impact of local volatility terms.

Our approach here is based on Watanabe's expansion [Wat87, KT03, Kaw02, Osa06] in conjunction with Itô-Taylor expansions of the underlying process's stochastic differential equation. In its essence, this technique bears similarity to the perturbative expansion analysis conducted by Hagan et. al. in [HKL02], Kawai [Kaw02], and Osajima [Osa06], in the sense that the formal expansion is done, effectively, in terms of short times to expiry or low volatility (albeit that, as is typical for asymptotic expansions, the final results work well also for large volatilities and times to expiry). Watanabe's expansion comprises the expansion of the vanilla option payoff function around Heavisides, Dirac, and derivatives of the Dirac function whence it works best for short to moderate times to maturity. The Watanabe expansion is only one part of the calculus, though, since it is only the final module in the evaluation of the vanilla option price. It requires, as an input, a decomposition of the driving stochastic process into an ordered series of noise terms of decreasing magnitude. The choice of this ordered series is entirely separate from the Watanabe expansion of the payoff, and one could use any suitable decomposition of the underlying process into a series of random terms whose individual distributions, conditional on all preceding terms, are analytically attainable. However, given that we are interested in solutions for a stochastic volatility model for which we have very limited knowledge of the process's distribution, we use standard Itô-Taylor expansions [KP99] of the stochastic differential equation of the underlying. The formal nature of Itô-Taylor expansions allows us to embed local volatility terms and the representation of volatility as a function of a standard Ornstein-Uhlenbeck process entirely transparently, whence we arrive at an expansion formula that depends solely on the local volatility term $f(\cdot)$ and the stochastic volatility term $g(\cdot)$ and their derivatives evaluated at the initial level of their respective arguments.

2 A hyperbolic-local hyperbolic-stochastic volatility model

After a long and careful selection process from all the possible mathematical formulations we could think of, we chose the new model's dynamics to be given by

$$dx = \sigma_0 \cdot f(x) \cdot g(y) \cdot dW \quad (1)$$

$$dy = -\kappa y \cdot dt + \alpha \sqrt{2\kappa} \cdot dZ \quad (2)$$

with correlated Brownian motions $\langle dW, dZ \rangle = \rho \cdot dt$, $y(0) = 0$ and the transformation functions

$$f(x) = \left[(1 - \beta + \beta^2) \cdot x + (\beta - 1) \cdot \left(\sqrt{x^2 + \beta^2(1 - x)^2} - \beta \right) \right] / \beta \quad (3)$$

$$g(y) = y + \sqrt{y^2 + 1} \quad (4)$$

wherein x is the financial observable that underlies the given derivatives pricing problem, y is the driver of volatility, and $\beta > 0$. Both $f(\cdot)$ and $g(\cdot)$ are hyperbolic versions of conic sections whence we refer to this model as the *hyperbolic-local hyperbolic-stochastic volatility model*, or the **Hyp-Hyp** model for short. We shall elaborate the reasons for the particular parametric choice in detail throughout the remainder of this article.

First, though, note that, in the following, we assume that $g(0) = 1$ which is obviously without loss of generality. Further, we assume that $x(0) = 1$ and $f(1) = 1$. That this is also without loss of generality can be seen as follows. Starting with an arbitrary local volatility parametrisation

$$dS = \tilde{\sigma} \cdot \tilde{f}(S) \cdot g(y) \cdot dW \quad (5)$$

and initial spot level $S(0) = S_0$, we can always choose

$$\sigma_0 := \tilde{\sigma} \cdot \tilde{f}(S_0) / S_0 \quad (6)$$

$$x := S / S_0 \quad (7)$$

$$f(x) := \tilde{f}(x \cdot S_0) / \tilde{f}(S_0) \quad (8)$$

to arrive at the formulation (1) with $x(0) = 1$ and $f(1) = 1$. The valuation of a plain vanilla call or put option on $S(T)$ struck at K then can be done by valuing the same type of option on $x(T)$ struck at

$$k := K / S_0 \quad (9)$$

and multiplying with S_0 .

2.1 Hyperbolic local volatility

The local volatility form (3) is designed to resemble the CEV functional form x^β of local volatility at the forward up to second order. Unlike the CEV or the displaced diffusion functional form of local volatility¹, though, the hyperbolic form (3) not only converges to zero for small x , but also has finite slope for $x \rightarrow 0$, as well as positive slope for $x \rightarrow \infty$. The specific shapes are demonstrated in figures 1 and 2. As a consequence of its zero value at zero, finite slope at zero, and finite positive slope for large x , when no stochasticity of volatility is present, the local volatility form (3) gives rise to finite positive implied volatilities for options for very high and very low strikes according to

$$\lim_{k \rightarrow 0} \hat{\sigma}_{\text{hyperbolic local}}(k) = \sigma_0 \cdot 1 / \beta \quad (10)$$

¹the latter being $\beta \cdot x + (1 - \beta) \cdot x_0$

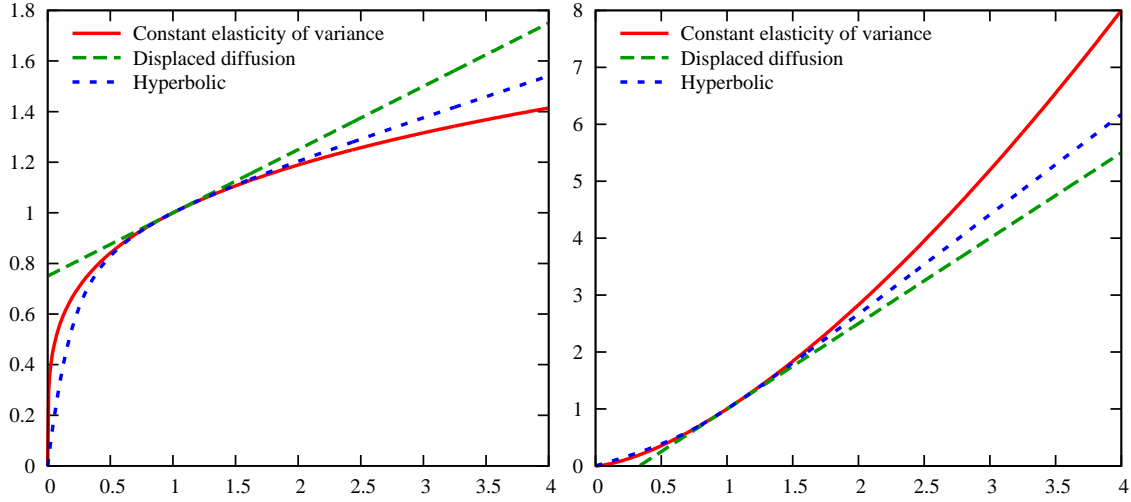


Figure 1: Absolute volatility for constant elasticity of variance (red, solid), displaced diffusion (green, long dashes), and hyperbolic (blue, short dashes) local volatility forms for $\beta = 1/4$ (left) and $\beta = 3/2$ (right).

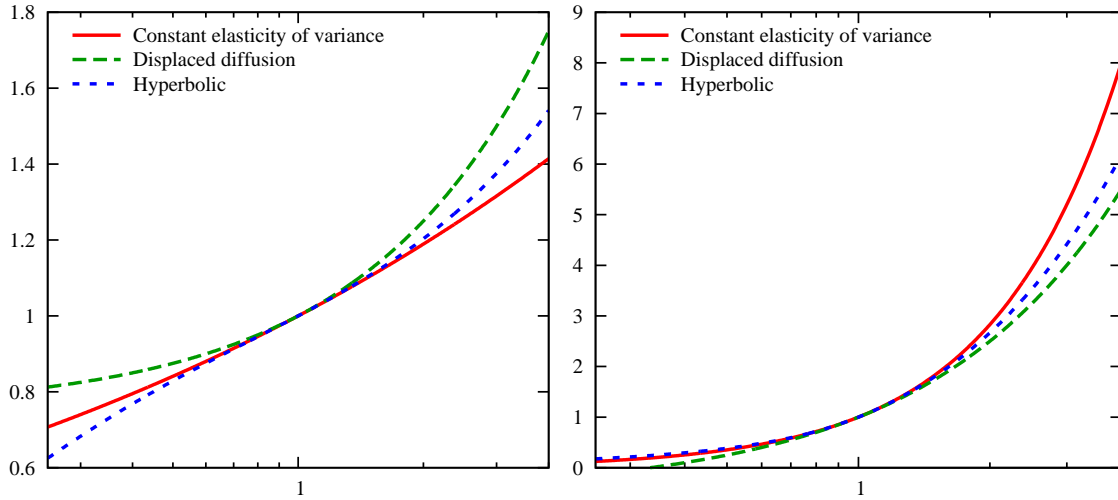


Figure 2: Absolute volatility on a logarithmic scale for constant elasticity of variance (red, solid), displaced diffusion (green, long dashes), and hyperbolic (blue, short dashes) local volatility forms for $\beta = 1/4$ (left) and $\beta = 3/2$ (right).

$$\lim_{k \rightarrow \infty} \hat{\sigma}_{\text{hyperbolic local}}(k) = \sigma_0 \cdot \left(\beta - 1 + \sqrt{1 + \beta^2} + \left(1 - \sqrt{1 + \beta^2} \right) / \beta \right). \quad (11)$$

An additional advantage of the finite slope near zero is that the local volatility form $f(x)$, unlike the CEV and displaced diffusion models, does not give rise to the underlying stochastic process attaining or even crossing zero, which is of considerable convenience for both numerical implementations as well as for the pricing of forward performance options. In essence, it is the careful selection of all of the above mentioned desirable traits of a parametric local volatility form, combined with an inspiration as to a *simple* yet suitable functional form, that gave rise to the function $f(x)$ given in equation (3). Further details of its derivation can be found in [Jäc06].

2.2 Hyperbolic stochastic volatility

The design of the stochastic volatility component of the new model was to balance the ideal to be as close as possible to the case of absolute volatility of volatility scaling like σ^p with $p \approx 1$ for the reasons mentioned in the introduction, whilst avoiding the fat tails of a log-normal distribution for

volatility in order to circumvent any moment explosions. A log-normal distribution for volatility is attained when $g_{\text{exp}}(y) = e^y$. The chosen hyperbolic function (4) shares level, slope, and curvature with the exponential function in $y = 0$, but differs as of the third derivative at $y = 0$ which is 0 for the hyperbolic $g(\cdot)$, as opposed to 1 for $g_{\text{exp}}(\cdot)$. The consequence of the difference in the higher order terms is that the hyperbolic form (4) grows less rapidly than the exponential function with increasing y , as well as decreases less strongly as $y \rightarrow -\infty$. This is shown in figure 3 where we have included the functional form $g_{\text{aff}}(y) = y + 1$ for comparison. In figure 4, we show the associated densities for

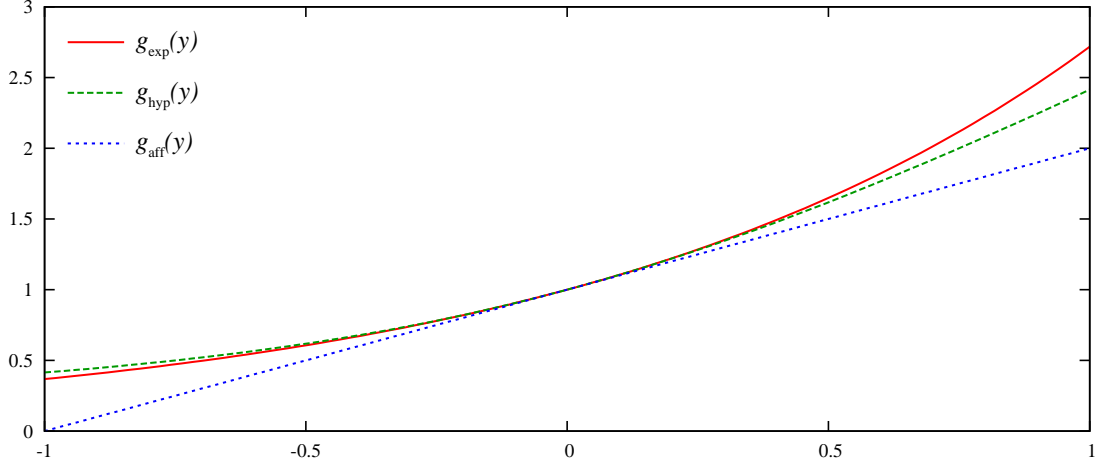


Figure 3: The exponential (e^y), hyperbolic ($y + \sqrt{y^2 + 1}$), and affine ($y + 1$) transformation functions.

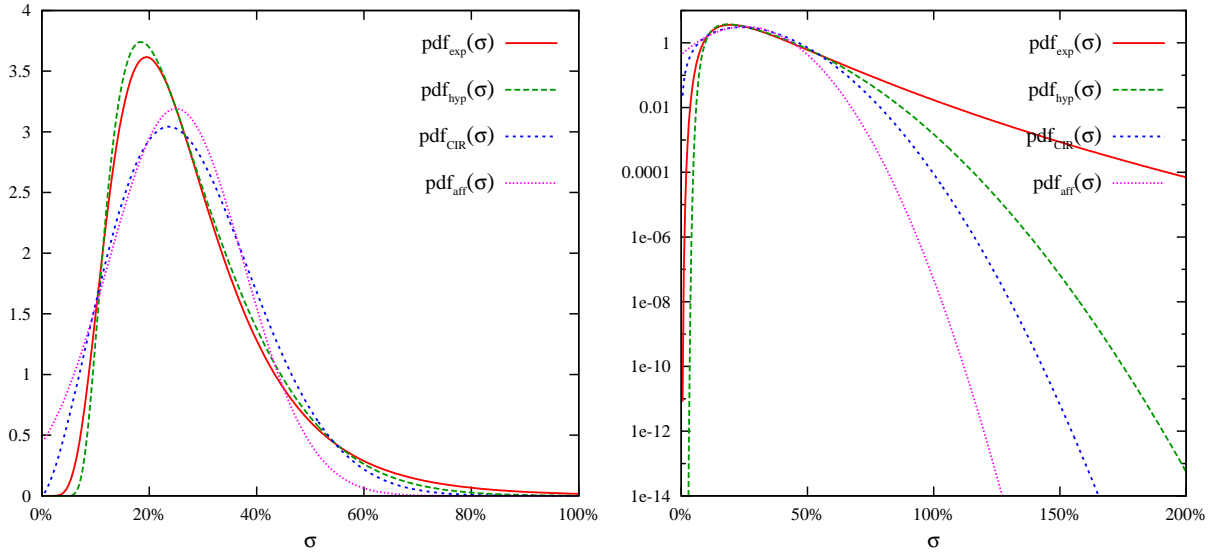


Figure 4: Densities of instantaneous volatility using the exponential, hyperbolic, and affine transformation of the driving Ornstein-Uhlenbeck process for $\sigma = \sigma_0 \cdot g(y)$ with $\sigma_0 = 25\%$, $\kappa = 1/2$, $T = 5$, $\eta = 1/2$, $\alpha = \eta/\sqrt{1 - e^{-2\kappa T}}$, plus the volatility density from a CIR process fitted to the hyperbolic density. The CIR process parameters are elaborated in the text. Note the distinctly different tails of the distributions.

$$\sigma = \sigma_0 \cdot g(y) \quad (12)$$

with $\sigma_0 = 25\%$, $\kappa = 1/2$, $T = 5$, $\eta = 1/2$, $\alpha = \eta/\sqrt{1 - e^{-2\kappa T}}$, together with the volatility density of a parameter-fitted CIR process given by

$$dv = \kappa_{\text{CIR}}(\theta_{\text{CIR}} - v)dt + \alpha_{\text{CIR}}\sqrt{v} \cdot dZ . \quad (13)$$

The CIR process parameters were chosen to match the initial level of volatility, the initial absolute value of volatility of volatility, the expectation at T , and the variance of the hyperbolic volatility process at T using the analytics in [And07, GJY99], and some numerical integration for the expectation of volatility, resulting in $v(0) = 0.0625$, $\alpha_{\text{CIR}} = 0.250847$, $\kappa_{\text{CIR}} = 0.389852$, and $\theta_{\text{CIR}} = 0.098938$. It can be seen in these figures that with respect to the tail behaviour of the densities, the fitted CIR process is approximately mid-way between a normal and a log-normal distribution, as one would expect. In addition, it can be seen that whilst the hyperbolic form gives rise to a density that, near the bulk of the distribution, resembles the log-normal distribution reasonably closely, it has much thinner tails for very low and very high values of volatility, which is precisely what we want to achieve with the selection of the functional form (4). Analytically, we can understand the thin tails of the hyperbolic volatility process by considering the solution of (4) and (12) for y :

$$y = \frac{1}{2} \cdot \left(\frac{\sigma}{\sigma_0} - \frac{\sigma_0}{\sigma} \right). \quad (14)$$

It follows straight away from this equation that in the limit of $\sigma \rightarrow \infty$, we have $\sigma \sim 2\sigma_0 \cdot y$, which means that the upper tail of the hyperbolic volatility form converges to that of a Gaussian distribution. Conversely, for $\sigma \rightarrow 0$, the relationship $\sigma \sim -\sigma_0/(2y)$ holds, i.e. we obtain the density of an inverse Gaussian near zero. The density of an inverse Gaussian near zero stands out as a function which not only in its value converges to zero as one approaches zero, but also in all of its derivatives. It is an *almost flat* function with zero value, slope, and curvature at zero. We consider the suppression of volatility levels near zero another desirable feature for economic reasons, which is why we find the hyperbolic form (4), when applied to a standard Ornstein-Uhlenbeck process, very well suited to represent market-realistic dynamics of instantaneous volatility.

3 Analytical approximation for implied volatilities

Having established which local-stochastic volatility model we find suitable for reasons of realism, numerical tractability, and financial appropriateness, we turn our attention to the important issue of calibration to market-observable implied volatilities for plain vanilla options. At the heart of this issue for any efficient risk-management and exotic derivative valuation is an analytical approximation for plain vanilla option prices, or better even, directly for implied volatilities. Following the lead of Watanabe and several follow-up publications [Wat87, KT03, Kaw03, Osa06], we have derived the generic formula

$$\hat{\sigma}(k, T) \approx \hat{\sigma}_{0,sl}(k, T) + \hat{\sigma}_{1,sl}(k, T) + \hat{\sigma}_{2,sl}(k, T) + \hat{\sigma}_{3,l}(k, T) + \hat{\sigma}_{4,l}(k, T) \quad (15)$$

with

$$\hat{\sigma}_{0,sl}(k, T) = \sigma_0 \quad (16)$$

$$\hat{\sigma}_{1,sl}(k, T) = \frac{z\sigma_0}{2\sqrt{T}} \cdot \left((f_1 - 1)\sigma_0 T + \sqrt{8}g_1\alpha\rho (\kappa T + e^{-\kappa T} - 1) / \left(\kappa^{3/2} T \right) \right) \quad (17)$$

$$\begin{aligned} \hat{\sigma}_{2,sl}(k, T) = & \frac{\sigma_0 \cdot e^{-2T\kappa}}{24T^3\kappa^3} \cdot \\ & \left[12\sqrt{2} \cdot e^{T\kappa} f_1 g_1 \alpha \kappa^{3/2} (e^{T\kappa}(T\kappa - 1) + 1) \rho \sigma_0 T^2 \right. \\ & - \kappa T \cdot \left[e^{2T\kappa} (f_1^2 - 2f_2 - 1) T^3 \kappa^2 \sigma_0^2 \right. \\ & \left. \left. - 6g_2\alpha^2 (2e^{2T\kappa} T^2 \kappa^2 - 5e^{2T\kappa} T\kappa + T\kappa - 8e^{T\kappa} + 6e^{2T\kappa} + 2) \rho^2 \right] \right] \end{aligned}$$

$$\begin{aligned}
& - 6g_1^2\alpha^2 \cdot \left[2e^{2T\kappa}T^3 (\rho^2 - 1) \kappa^3 + T^2 (-9e^{2T\kappa}\rho^2 + \rho^2 + 5e^{2T\kappa} - 1) \kappa^2 \right. \\
& \quad \left. - 2(e^{T\kappa} - 1) T (-7e^{T\kappa}\rho^2 + \rho^2 + 3e^{T\kappa} - 1) \kappa - 4(e^{T\kappa} - 1)^2 \rho^2 \right] \\
& + z^2 \cdot \left[-12\sqrt{2} \cdot e^{T\kappa}g_1\alpha\kappa^{3/2} (e^{T\kappa}(T\kappa - 1) + 1) \rho\sigma_0T^2 \right. \\
& \quad \left. - \kappa T \left[e^{2T\kappa} (2f_1^2 + 6f_1 - 4f_2 - 8) T^3\kappa^2\sigma_0^2 \right. \right. \\
& \quad \quad \left. \left. - 6g_2\alpha^2 (4e^{2T\kappa}T\kappa + 8e^{T\kappa} - 6e^{2T\kappa} - 2) \rho^2 \right] \right. \\
& \quad \left. - 6g_1^2\alpha^2 \left[T^2 (12e^{2T\kappa}\rho^2 - 4e^{2T\kappa}) \kappa^2 + 8(e^{T\kappa} - 1)^2 \rho^2 \right. \right. \\
& \quad \quad \left. \left. - 2(e^{T\kappa} - 1) T (11e^{T\kappa}\rho^2 - \rho^2 - 3e^{T\kappa} + 1) \kappa \right] \right] \quad (18)
\end{aligned}$$

$$\begin{aligned}
\hat{\sigma}_{3,l}(k, T) &= \frac{T^{3/2}z\sigma_0^4}{48} \cdot \left[-f_1^3 + f_1^2 + (2f_2 + 3)f_1 - 2f_2 + 2f_3 - 3 \right. \\
& \quad \left. + 2z^2 \cdot \left[f_1^3 + f_1^2 + (4 - 2f_2)f_1 - 2f_2 + f_3 - 6 \right] \right] \quad (19)
\end{aligned}$$

$$\begin{aligned}
\hat{\sigma}_{4,l}(k, T) &= -\frac{T^2\sigma_0^5}{5760} \cdot \\
& \left[8 \cdot z^4 \cdot \left(19f_1^4 + 15f_1^3 + (20 - 46f_2)f_1^2 + 6(3f_3 - 5f_2 + 15) f_1 \right. \right. \\
& \quad \left. \left. - 40f_2 + (16f_2^2 + 15f_3) - 6f_4 - 144 \right) \right. \\
& - 2 \cdot z^2 \cdot \left[11f_1^4 + 30f_1^3 + (20 - 44f_2)f_1^2 + 6(12f_3 - 10f_2 - 45) f_1 \right. \\
& \quad \left. + 140f_2 + (44f_2^2 - 60f_3) + 36f_4 + 209 \right] \\
& \left. - 3 \cdot (3f_1^4 - 2(6f_2 + 5)f_1^2 + 16f_3f_1 + 12f_2^2 + 20f_2 + 8f_4 + 7) \right] \cdot \quad (20)
\end{aligned}$$

and

$$z := (k - 1) / (\sigma_0\sqrt{T}) \quad (21)$$

as well as

$$\begin{aligned}
f_j &= f^{(j)}(1), \quad \text{for } j = 1, 2, 3, 4 \\
g_k &= g^{(k)}(0), \quad \text{for } k = 1, 2
\end{aligned} \quad (22)$$

for *any* stochastic volatility model of the form given by equations (1) and (2). The details of the derivation can be found in [Kah07]. Specifically for the hyperbolic-local hyperbolic-stochastic volatility model, this means

$$\begin{aligned}
f_1 &= \beta, & f_2 &= \beta(\beta - 1), & f_3 &= -3\beta(\beta - 1), & f_4 &= -3\beta(\beta - 1)(\beta^2 - 4), \\
g_1 &= 1, & g_2 &= 1 & .
\end{aligned} \quad (23)$$

The price of a vanilla option is then given by

$$v(S_0, K, T) = S_0 \cdot \mathbf{B}(1, k, \hat{\sigma}, T) \quad (24)$$

with $\hat{\sigma}$ given by equation (15), and $\mathbf{B}(F, K, \hat{\sigma}, T)$ being Black's [Bla76] formula. It should be noted that specifically for the hyperbolic stochastic volatility form (4) the formula (15) is accurate up to third order deviations of the volatility driver from zero even though it only contains terms up to g_2 . This is by virtue of the fact that the function $g(\cdot)$ as given in (4) has vanishing coefficient $g_3 = g'''(0)$ which is another advantage of this particular choice for $g(\cdot)$.

3.1 Scaling correction

Comparing the asymptotic approximation of the implied volatility in the *Hyp-Hyp* model with the correct implied volatility given via a Monte-Carlo simulation of the stochastic differential equations (1) and (2) reveals that formula (15) is less accurate for long times to maturity. For the hyperbolic local and stochastic volatility model the Watanabe expansion typically underestimates the true implied volatility level.

In order to address the problem of not matching the implied volatility at-the-money, we are looking for a different asymptotic approximation method to rescale the implied volatility formula (15). Since the Watanabe approximation provides accurate results for short times to expiry, we ideally need a method which works for long times to maturity. The asymptotic fast mean-reverting approximation of Fouque et al. [FPS00] matches this criterium. It is given as a function of the *log-moneyness-to-maturity-ratio* $\ln(K/F)/T$:

$$\hat{\sigma}_{\text{Fouque}} = a \cdot \frac{\ln(K/F)}{T} + b + \mathcal{O}(1/\kappa) ; \quad (25)$$

with auxiliary parameters

$$a = \frac{-V_2}{2\hat{\sigma}_{\text{RMS}}^3}, \quad \text{and} \quad b = \hat{\sigma}_{\text{RMS}} - \frac{V_2}{4\hat{\sigma}_{\text{RMS}}}, \quad (26)$$

where $\hat{\sigma}_{\text{RMS}}$ is the root-mean square volatility and

$$V_2 = \frac{-2\rho}{\alpha\sqrt{2\kappa}} \cdot \langle G \cdot (g^2 - \langle g^2 \rangle_\varphi) \rangle_\varphi. \quad (27)$$

Here $\langle \cdot \rangle_\varphi$ denotes the integration with respect to the stationary distribution of the underlying Ornstein-Uhlenbeck process (2) and G is the primitive of the hyperbolic transformation function (4). In contrast to the exponential transformation function, it is not possible to find a closed form solution for (27) for the hyperbolic case (4). Still, assuming $\alpha < 1$, we have been able to derive the approximation [Kah07, sec. 4.2.7]

$$\begin{aligned} \hat{\sigma}_{\text{Fouque}}(F, K, T) \approx \sigma_0 \cdot & \sqrt{\frac{(e^{-2T\kappa} - 1)\alpha^2}{T\kappa} + 2\alpha^2 + 1} - \frac{\alpha(\alpha^4 - 7\alpha^2 - 1)\rho\sigma_0^2}{\sqrt{2\left(\frac{(e^{-2T\kappa} - 1)\alpha^2}{T\kappa} + 2\alpha^2 + 1\right)\kappa}} \\ & - \frac{\sqrt{2} \cdot T\alpha(\alpha^4 - 7\alpha^2 - 1)\kappa\rho}{((2 \cdot T\kappa + e^{-2T\kappa} - 1)\alpha^2 + T\kappa)^{3/2}} \cdot \ln\left(\frac{F}{K}\right) \end{aligned} \quad (28)$$

for Fouque's generic formula (25) when $g(\cdot)$ is given by (4).

One of the shortcomings of Fouque's formula for the use of implied volatility approximations across the whole surface is that it reflects the strike dependence merely by a term proportional to $\ln(F/K)$. However, at-the-money, it is asymptotically exact for large $\kappa \cdot T$, and it is this latter fact that we use for an ad-hoc scaling correction of the level of the implied volatility formula (15). The idea is to set

$$\hat{\sigma}_{\text{Hyp-Hyp}}(k, T) = \hat{\sigma}(k, T) \cdot \left(\frac{\hat{\sigma}_{\text{Fouque,ATM}}(T)}{\hat{\sigma}_{\text{vol,ATM}}(T)} (1 - h(T)) + h(T) \right), \quad (29)$$

where $\hat{\sigma}_{\text{Fouque,ATM}} = \hat{\sigma}_{\text{Fouque}}(F, F, T)$ and $\sigma_{\text{vol,ATM}}$ denotes the implied volatility of the Watanabe approximation (15) at-the-money. The transformation function $h : \mathbb{R} \rightarrow [0, 1]$ is required to be monotonically decaying with boundary conditions $h(0) = 1$ and $\lim_{x \rightarrow \infty} h(x) = 0$. A function satisfying these properties is the exponential form

$$h_{\text{exponential scaling}}(T) = \exp(-\kappa \cdot T), \quad (30)$$

where the parameter κ is added to weight the scaling. The exponential function decays rapidly when we increase time to maturity, such that the at-the-money volatility is relatively early governed by the

fast mean-reverting expansion of Fouque et al. [FPS00], and we show in figure 5 an example that this choice of $h(\cdot)$ is generally not accurate enough.

To overcome this problem we want to choose a parametric form for the scaling which does not decay as fast as the exponential function. Here again the hyperbolic function comes to our rescue:

$$h_{\text{hyperbolic scaling}}(T) = g\left(-\sqrt{\alpha \cdot \kappa \cdot T}\right) \quad (31)$$

with the hyperbolic transformation function g as defined in (4). Note that in contrast to the exponential scaling in (30) we use a slightly different parameter combination here. This is motivated by the fact that we do not want the at-the-money volatility to approach the Fouque asymptotics too quickly. Furthermore, we add the parameter α into the scaling since the Watanabe approximation is particularly accurate for small values of α such that we need less scaling. In addition to that, we compare with

$$h_{\text{exponential scaling (second)}}(T) = \exp\left(-\sqrt{\alpha \cdot \kappa \cdot T}\right). \quad (32)$$

We show the different scalings in figure 5 where we can also see that the Watanabe approximation typically underestimates the implied volatility whilst the formula of Fouque overestimates the true level of volatility. We give further evidence of the effectiveness of the hyperbolic scaling formula later on in section 5 where we show the calibration results to market given implied volatility surfaces.

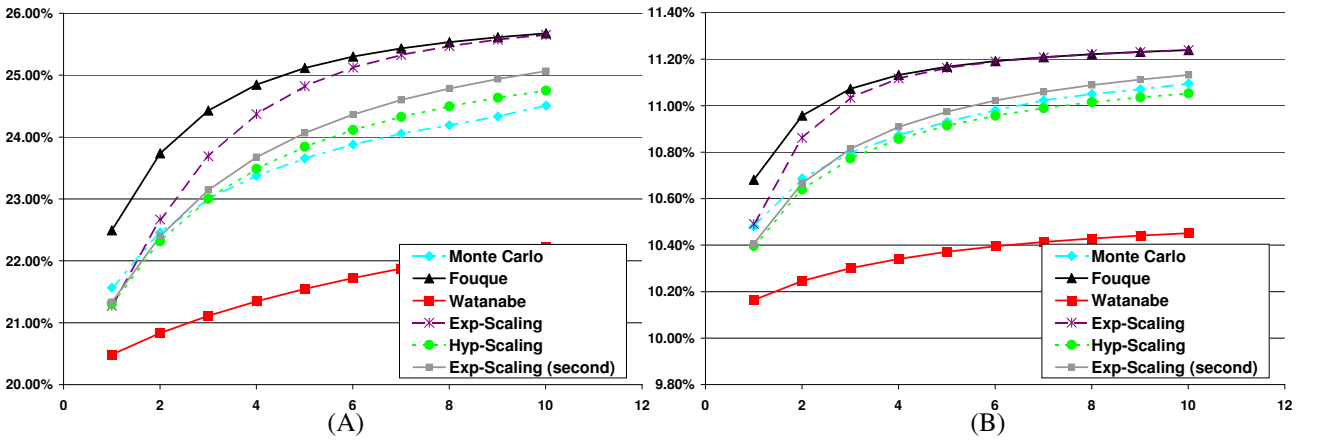


Figure 5: At-the-money volatilities for the Watanabe and Fouque approximation over time to maturity with different scalings *Exp-Scaling* (30), *Hyp-Scaling* (31) as well as *Exp-Scaling (second)* (32). The parameter configuration is given as (A): $\alpha = 3/5$, $\beta = 1$, $\kappa = 1/2$, $\sigma = 1/5$, $\rho = 0$ as well as (B): $\alpha = 2/5$, $\beta = 1$, $\kappa = 1$, $\sigma = 1/10$, $\rho = -1/2$. The Monte Carlo result is calculated via a *log-Euler scheme* (53) with a stepsize of $\Delta t = 1/16$ and $N = 2^{16} - 1$ paths constructed using low-discrepancy Sobol' numbers in conjunction with a Brownian bridge.

3.2 Time dependent instantaneous volatility

The implied volatility parametrisation (15) of the *Hyp-Hyp* model is a function of the model parameters $\Omega_{\text{Hyp-Hyp}} = \{\sigma_0, \alpha, \beta, \rho, \kappa\}$ as well as the relative strike k and the time to maturity T . In order to calibrate the model to market implied volatility surfaces one may want to find the set $\Omega_{\text{Hyp-Hyp}}$ which minimizes the calibration error over a set of strikes $\mathcal{K} = \{k_1, k_2, \dots, k_N\}$ and maturities $\mathcal{T} = \{T_1, T_2, \dots, T_M\}$

$$\sum_{\mathcal{K}, \mathcal{T}} \|\hat{\sigma}_{\text{Market}}(k_i, T_j) - \hat{\sigma}_{\text{Hyp-Hyp}}(k_i, T_j)\|. \quad (33)$$

In order to replicate a term-structure of market implied volatilities $\hat{\sigma}_{\text{Market}}(k, \cdot)$ over time, we need to generalise the Watanabe approximation to allow for time dependent instantaneous volatility σ_0 . It

turns out that one can approximate the constant volatility σ_0 at time T with the corresponding realised variance

$$\|\sigma\|_2 = \sqrt{\frac{1}{T} \int_0^T \sigma_0(s)^2 ds}. \quad (34)$$

This added flexibility allows to calibrate the *Hyp-Hyp* model efficiently and accurately to market implied volatility surfaces. We show in section 5, that using the realised variance (34) works remarkably well if we compare the implied volatility formula (15) with results obtained from Monte-Carlo simulations.

3.3 SVI projection for wing adjustments

The limiting behaviour of all consistent implied volatility formulae for large log-strikes must be such that implied variance is affine in the logarithm of the strike. On the search for a suitable implied variance parametrisations, Jim Gatheral came up with the *Stochastic Volatility Inspired* [Gat04, Gat06] functional form:

$$\hat{\sigma} = \sqrt{a_{\text{SVI}} + b_{\text{SVI}} \cdot \left(\rho_{\text{SVI}} (\ln k - m_{\text{SVI}}) + \sqrt{(\ln k - m_{\text{SVI}})^2 + \sigma_{\text{SVI}}^2} \right)}, \quad (35)$$

whereby

- a_{SVI} gives the overall level of variance
- b_{SVI} gives the angle between the left and right asymptotes
- σ_{SVI} determines how smooth the vertex is
- ρ_{SVI} determines the orientation of the graph
- m_{SVI} translates the graph

Since the Watanabe expansion (15) is a fourth order polynomial in K/F , it is guaranteed to lead to problems for extremely far out of the money options. We therefore use a projection onto the SVI parametric form by expanding both the SVI variance and the squared Watanabe implied volatility form up to fourth order in $\ln k$, and matching coefficients:

$$\hat{\sigma}^2(k) = v_0 + v_1 \cdot \ln k + v_2 \cdot (\ln k)^2 + v_3 \cdot (\ln k)^3 + v_4 \cdot (\ln k)^4 + \mathcal{O}((\ln k)^5) \quad (36)$$

This gives us the *analytical SVI projection*

$$\begin{aligned} a_{\text{SVI}} &= v_0 + \frac{v_1 v_2 v_3 - 2v_2^3}{5v_3^2 - 4v_2 v_4} & b_{\text{SVI}} &= \frac{v_2 |v_2| \sqrt{5v_3^2 - 4v_2 v_4}}{2(v_3^2 - v_2 v_4)} \\ \sigma_{\text{SVI}}^2 &= \frac{4v_2^2 (v_3^2 - v_2 v_4)}{(5v_3^2 - 4v_2 v_4)^2} & \rho_{\text{SVI}} &= \frac{v_2^2 v_3 + 2v_1 (v_3^2 - v_2 v_4)}{v_2 |v_2| \sqrt{5v_3^2 - 4v_2 v_4}} \\ m_{\text{SVI}} &= \frac{v_2 v_3}{5v_3^2 - 4v_2 v_4}. \end{aligned} \quad (37)$$

Complex arithmetic can be avoided by combining (35) and (37) to

$$\hat{\sigma}^2 = a_{\text{SVI}} + \left(v_1 + \frac{v_2^2 v_3}{2(v_3^2 - v_2 v_4)} \right) \cdot (\ln k - m_{\text{SVI}}) + \frac{v_2 |v_2| \sqrt{(5v_3^2 - 4v_2 v_4)} (\ln k - 2m_{\text{SVI}}) \ln k + v_2^2}{2(v_3^2 - v_2 v_4)} \quad (38)$$

with a_{SVI} and m_{SVI} as in (37). For the sake of brevity, we omit the explicit forms for v_0 , v_1 , v_2 , v_3 , v_4 , though, it should be straightforward for the knowledgeable reader to square the analytical formula (15), expand it in $\ln k$ around zero to fourth order, and extract the resulting polynomial's coefficients.

Whilst the formulæ (37) are not explicitly guaranteed to give real valued answers, we found in practice that complex values result only in very unusual circumstances. Even when this happens, in our experience, the real parts work very well as an initial guess for any of the commonly available fitting procedures [PTVF92], and the final match was always of good quality for all scenarios we analyzed throughout data from interest rate, equity, commodity, foreign exchange, and inflation derivatives markets. We conclude this section with some examples for the (analytical) SVI projection for strongly skewed implied volatilities in figures 6 and 7.

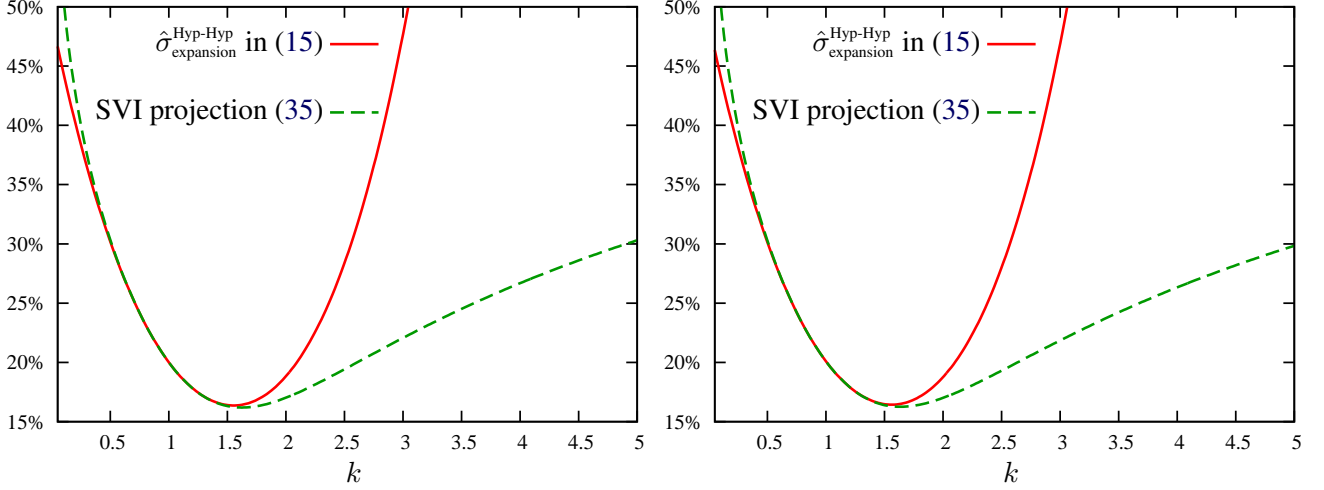


Figure 6: Implied volatilities from formulæ (15) and (35) for $\sigma_0 = 1/5$, $\beta = 1/2$, $\kappa = 1/10$, $\alpha = 1/(3\sqrt{2\kappa})$, $\rho = -1/2$, and (left) $T = 1/52$ and (right) $T = 1/2$.

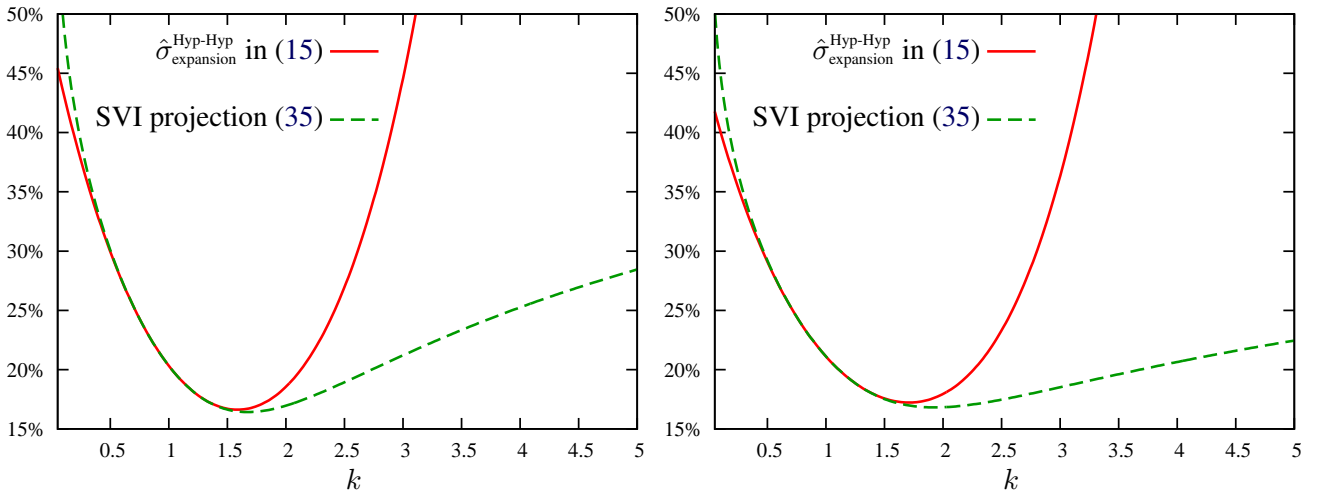


Figure 7: Implied volatilities from formulæ (15) and (35) for $\sigma_0 = 1/5$, $\beta = 1/2$, $\kappa = 1/10$, $\alpha = 1/(3\sqrt{2\kappa})$, $\rho = -1/2$, and (left) $T = 2$ and (right) $T = 10$.

3.4 Delta

The rescaling of parameters and stochastic variables in equations (6) to (9) was introduced for a simplification of the subsequent valuation expressions. However, when the sensitivity of an option price with respect to the underlying is to be computed, one has to be aware of the fact that the rescaled local volatility parameters may themselves be subject to change as the underlying spot value is shifted, in accordance with the original local volatility model assumption.

Taking the complete differential of the option valuation formula (24) with respect to S_0 gives us

$$\frac{dv}{dS_0} = \mathbf{B} + S_0 \cdot \partial_{S_0} k \cdot \partial_k \mathbf{B} + S_0 \cdot \partial_{\hat{\sigma}} \mathbf{B} \cdot \left[\partial_{S_0} \sigma_0 \cdot \partial_{\sigma_0} \hat{\sigma} + \partial_{S_0} k \cdot \partial_k \hat{\sigma} + \sum_{n=1}^4 \partial_{S_0} f_n \cdot \partial_{f_n} \hat{\sigma} \right], \quad (39)$$

with $\mathbf{B} = \mathbf{B}(1, k, \hat{\sigma}, T)$ and $\hat{\sigma} = \hat{\sigma}(\sigma_0, k, T, f_1, f_2, f_3, f_4, \dots)$. Starting with equation (8), straightforward calculation of the required derivatives yields

$$f_n = S_0^n \cdot \tilde{f}^{(n)}(S_0) / \tilde{f}(S_0) \quad (40)$$

whence

$$\partial_{S_0} f_n = \partial_{S_0} \left(S_0^n \cdot \tilde{f}^{(n)}(S_0) / \tilde{f}(S_0) \right) = (f_{n+1} + f_n(n - f_1)) / S_0. \quad (41)$$

Equally, starting from (6), we obtain

$$\partial_{S_0} \sigma_0 = \partial_{S_0} \left(\tilde{\sigma} \cdot \tilde{f}(S_0) / S_0 \right) = \tilde{\sigma} \cdot \left(\tilde{f}'(S_0) / S_0 - \tilde{f}(S_0) / S_0^2 \right) = \sigma_0 \cdot (f_1 - 1) / S_0. \quad (42)$$

Substituting this into (39), we obtain the generic formula for the option's delta:

$$\frac{dv}{dS_0} = \mathbf{B} - k \cdot \partial_k \mathbf{B} + \partial_{\hat{\sigma}} \mathbf{B} \cdot \left[\sigma_0 \cdot (f_1 - 1) \cdot \partial_{\sigma_0} \hat{\sigma} - k \cdot \partial_k \hat{\sigma} + \sum_{n=1}^4 (f_{n+1} + f_n \cdot (n - f_1)) \cdot \partial_{f_n} \hat{\sigma} \right]. \quad (43)$$

As an example, consider the simple displaced diffusion model [Rub83]. In this case, we have

$$\tilde{f}^{\text{DD}}(S) = \beta \cdot S + (1 - \beta) \cdot S_0 \quad f^{\text{DD}}(x) = \beta \cdot x + (1 - \beta) \quad g^{\text{DD}}(y) = 1 \quad (44)$$

$$f_1^{\text{DD}} = \beta \quad f_2^{\text{DD}} = f_3^{\text{DD}} = f_4^{\text{DD}} = 0 \quad g_1^{\text{DD}} = g_2^{\text{DD}} = 0. \quad (45)$$

The exact call option value (without discounting) is

$$v^{\text{DD}} = \mathbf{B}(S + X, K + X, \beta\sigma, T) \quad \text{with} \quad X = (1 - \beta)S_0 / \beta. \quad (46)$$

The implied volatility according to (15) is

$$\hat{\sigma}(k) = \sigma_0 \left[1 + \frac{(1-\beta)}{2} \cdot \left(\frac{1+\beta}{12} \sigma_0^2 T - \left(1 + \frac{3-\beta^2}{24} \sigma_0^2 T \right) (k - 1) \right. \right. \\ \left. \left. + \left(\frac{4+\beta}{12} + \frac{209-\beta(61+\beta(41+11\beta))}{2880} \sigma_0^2 T \right) (k - 1)^2 \right) \right] + \mathcal{O}(\sigma_0^5), \quad (47)$$

and this is in exact agreement with a direct Taylor expansion (which is possible for this model). The exact call option delta (without discounting) is

$$\Delta^{\text{DD}} = \Phi \left(\ln \left(\frac{(S+X)}{(K+X)} \right) / (\beta\sigma\sqrt{T}) + \beta\sigma\sqrt{T} / 2 \right). \quad (48)$$

For the hyperbolic-local hyperbolic-stochastic volatility model, we obtain for the coefficient f_5 needed for the calculation of $d_{S_0} v$:

$$f_5 = 15\beta(\beta - 1)(3\beta^2 - 4). \quad (49)$$

The remaining terms $\partial_{\sigma_0} \hat{\sigma}$, $\partial_k \hat{\sigma}$, and $\partial_{f_n} \hat{\sigma}$ have to be determined from the implied volatility formula (15). This can either be done analytically, or, for the sake of speedy implementation and flexibility with respect to the choice of scaling correction as discussed in section 3.1, one can also use centred finite differencing to compute these terms.

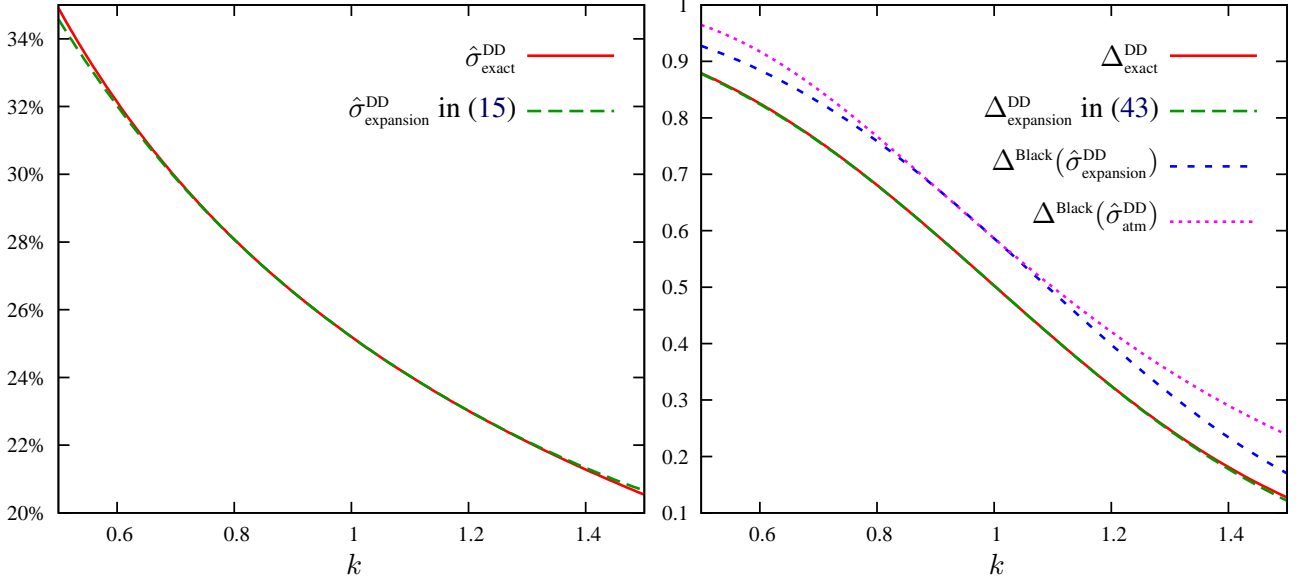


Figure 8: Left: implied volatility from formula (15) for the displaced diffusion model in comparison with exact solution. Right: delta for the displaced diffusion model as given by (48), the approximation (43), Black's delta using the implied volatility given by (15), and Black's delta using the at-the-money volatility. The parameters were $\sigma_0 = 1/4, \beta = 1/32, T = 3$.

4 Numerical implementation

The pricing of non-vanilla derivatives within the *Hyp-Hyp* model by the aid of Monte Carlo simulations is facilitated by the fact that volatility is given by a transformed *Ornstein-Uhlenbeck* [UO30] process with solution

$$y_t = e^{-\kappa t} \left(y_0 + \alpha \sqrt{2\kappa} \int_0^t e^{\kappa u} dZ_u \right), \quad (50)$$

where y_0 denotes the initial value of y . Thus y_t is Gaussian distributed

$$y_t \sim \mathcal{N} \left(y_0 \cdot e^{-\kappa t}, \alpha^2 (1 - e^{-2\kappa t}) \right). \quad (51)$$

With respect to the financial underlying, it is useful to consider the formal solution to (1) in logarithmic coordinates:

$$\ln x_t = \ln x_0 - \frac{1}{2} \sigma_0^2 \int_0^t \left(\frac{f(x_s)}{x_s} g(y_s) \right)^2 ds + \sigma_0 \int_0^t \left(\frac{f(x_s)}{x_s} g(y_s) \right) dW(s), \quad (52)$$

One can approximate (52) on a given time interval $[t_n, t_{n+1}]$ by the Euler-Maruyama scheme

$$\ln x_{t_{n+1}} = \ln x_{t_n} - \frac{1}{2} \sigma_0^2 \left(\frac{f(x_{t_n})}{x_{t_n}} g(y_{t_n}) \right)^2 \cdot \Delta t_n + \sigma_0 \cdot \frac{f(x_{t_n})}{x_{t_n}} g(y_{t_n}) \Delta W_n, \quad (53)$$

whereby $\Delta t_n = t_{n+1} - t_n$ and $\Delta W_n \sim \mathcal{N}(0, \Delta t_n)$. And herein lies one of the reasons for the specific choice for $f(\cdot)$ given by (3): the scheme (53) remains positive without any further ado by the simple fact that for $x \rightarrow 0$, we have

$$f(x)/x = \left(1 + \frac{\beta-1}{2\beta} \cdot x + \frac{\beta-1}{2\beta} \cdot x^2 + \frac{(\beta-1)(4\beta^2-1)}{8\beta^3} \cdot x^3 + \mathcal{O}(x^4) \right) / \beta. \quad (54)$$

In contrast, the functional form for $f(\cdot)$ for the CEV (x^β) or displaced diffusion ($\beta x + (1 - \beta)x_0$) models lead, for $\beta < 1$ (as is usually the case in the market), to diverging terms in absolute local volatility for small values of x which require special treatment in any numerical implementation.

Having said that, we should issue one caveat: whilst the scheme (53) is *analytically* guaranteed to stay away from zero, *numerically* the term $\ln x_t$ can, for $\beta \ll 1$, become so negative that the value for x_t itself is numerically indistinguishable from zero. This, however, is a feature also shared by geometric Brownian motion when $\sigma \cdot \sqrt{T} \gg 1$. Still, one ought to be aware of this issue when pricing exotic options which depend on the reciprocal of the underlying such as cliquets or CPPIs.

5 Accuracy of the approximation

We show in figure 9 comparisons of the numbers given by the asymptotic implied volatility formula (15) (which is quartic in k) with results from a Monte-Carlo simulation of the underlying dynamics (1) and (2). We consider the scaling-corrected asymptotic formula to be well within the accuracy required for all practical purposes for at-the-money options. With respect to its slight divergence from the true value for very far out-of-the-money options, it is worth bearing in mind that calibration is typically only required to be highly accurate within a range that is comparatively close to the money, especially since far out-of-the-money options typically have extremely little time value anyway. Nevertheless, when a better match of the stochastic volatility model's implied volatility behaviour in the wings is required, it is straightforward to fit a suitable functional form for implied volatility to our asymptotic quartic form up to fourth order near the money, and infer the behaviour far away from the money from the chosen functional form. When the selected function represents generic stochastic volatility model behaviour well, this typically results in very good matches even for very far out of the money options. Since the details of such an extension are beyond the scope of this article, we refer the reader to the generic forms suggested in [Gat04, Gat06]. In figure 10,

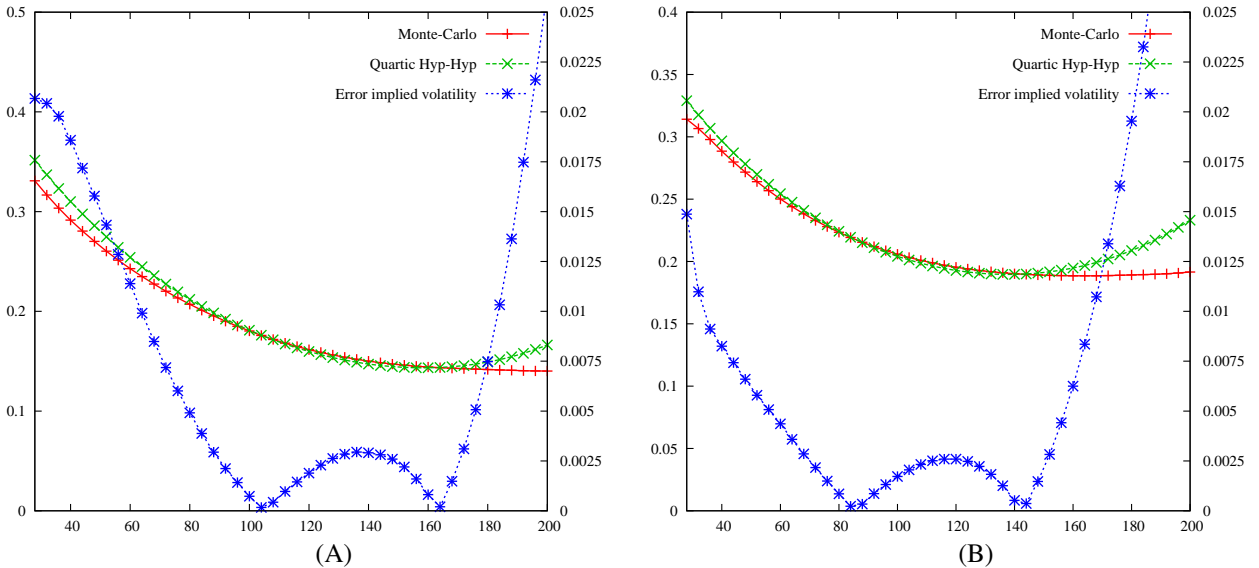


Figure 9: Comparison of the implied volatility approximation (15) with scaling function (31) with the results of a Monte-Carlo simulation, using the log-Euler scheme (53) with a stepsize of $\Delta t = 1/10$ and $N = 2^{20} - 1$ paths constructed using low-discrepancy Sobol' numbers in conjunction with a Brownian bridge. The parameter configuration is given as (A): $\beta = 3/10$, $\alpha = 1/2$, $\kappa = 1$, $\sigma_0 = 4/25$, $\rho = -1/2$, and time to maturity $T = 3$ as well as (B): $\beta = 7/10$, $\alpha = 3/10$, $\kappa = 1$, $\sigma_0 = 1/5$, $\rho = -3/10$, and time to maturity $T = 1$.

we show the impact of using the realised variance (34) within the asymptotic implied volatility formula (15) to cater for a time dependence of the instantaneous volatility level parameter $\sigma_0(t)$. We see that neither an upward nor a downward movement of instantaneous volatility leads to a deterioration of the approximation quality.

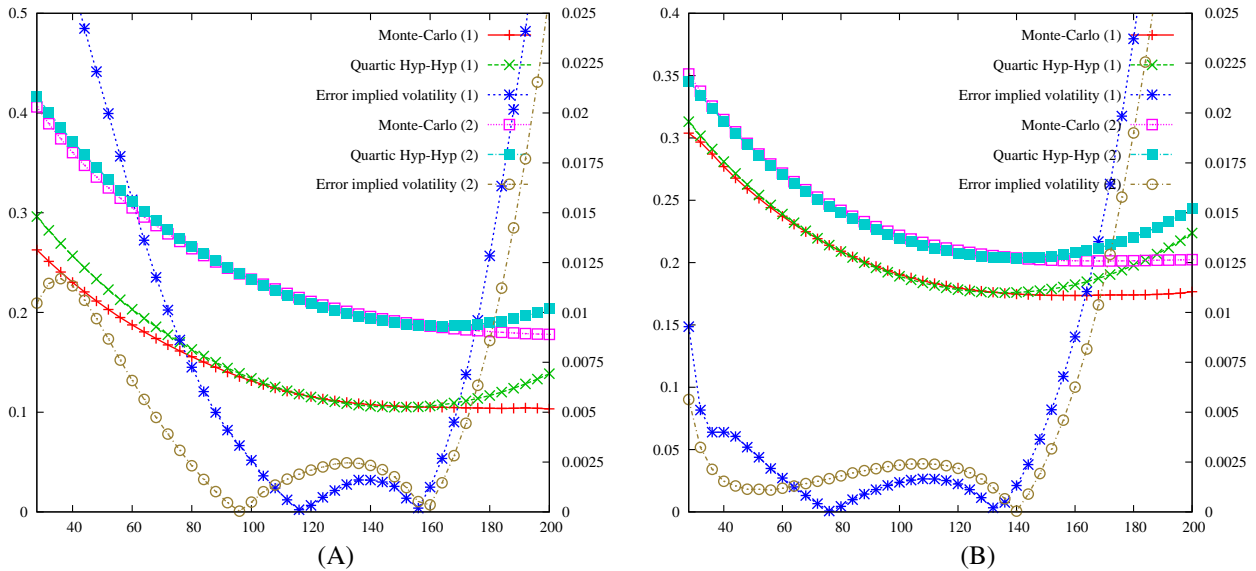


Figure 10: Comparison of the implied volatility approximation (15) with scaling function (31) with the results of a Monte-Carlo simulation, using the log-Euler scheme (53) with a stepsize of $\Delta t = 1/10$ and $N = 2^{20} - 1$ paths constructed using low-discrepancy Sobol' numbers in conjunction with a Brownian bridge. The parameter configuration is given as (A): $\beta = 3/10$, $\alpha = 1/2$, $\kappa = 1$, $\sigma_{(2)/(1)}(t) = 4/25 \pm 3/100 \cdot t$, $\rho = -1/2$, and time to maturity $T = 3$ as well as (B): $\beta = 7/10$, $\alpha = 3/10$, $\kappa = 1$, $\sigma_{(2)/(1)}(t) = 1/5 \pm 3/100 \cdot t$, $\rho = -3/10$, and time to maturity $T = 1$.

6 Conclusion

We have presented a new stochastic volatility approach whose starting point was to *design* a model by *choosing* desirable features, as opposed to the more conventional approach to select equations and accomodate undesirable features as a price to pay for the analytical tractability. Since there is no such thing as a free lunch, we had in turn to invoke more complicated means in order to arrive at analytical approximations for plain vanilla option calibration equations for the new *Hyp-Hyp* model. However, given that we had the liberty to genetically engineer a model that is in our opinion a better compromise between financial suitability and numerical implementation and performance requirements for the valuation of exotic options, we considered the investment in the analysis worth while, and we presented the results and demonstrated their accuracy. In addition to the introduction of the new model and its analytical vanilla option pricing approximations we also produced some generic analytical results for the implied volatility for *any* parametric-local-and-stochastic-volatility model by the aid of rather involved calculations based on Watanabe's theorem whose details we omitted in this article for the sake of brevity.

References

- [AA02] L. Andersen and J. Andreasen. Volatile volatilities. *Risk*, 15(12):163–168, 2002.
- [AL05] M. Atlan and B. Leblanc. Hybrid Equity credit modelling. *Risk*, 8(8):18, 2005.
- [AMST07] H. Albrecher, Ph. Mayer, W. Schoutens, and J. Tistaert. The Little Heston Trap. *Wilmott*, January:83–92, 2007.
- [And07] L. B. Andersen. Efficient Simulation of the Heston Stochastic Volatility Model. *SSRN eLibrary*, 2007. ssrn.com/paper=946405.
- [AP04] L. Andersen and V. Piterbarg. Moment Explosions in Stochastic Volatility Models. Technical report, Bank of America, 2004. ssrn.com/abstract=559481.

- [Bla76] F. Black. The pricing of commodity contracts. *Journal of Financial Economics*, 3:167–179, 1976.
- [CR76] J. C. Cox and S. A. Ross. The valuation of options for alternative stochastic processes. *Journal of Financial Economics*, 3:145–166, March 1976.
- [For06] M. Forde. Tail asymptotics for diffusion processes, with applications to local volatility and CEV-Heston models. *ArXiv Mathematics e-prints*, August 2006. xxx.lanl.gov/PS_cache/math/pdf/0608/0608634v6.pdf.
- [FPS00] J.-P. Fouque, G. Papanicolaou, and K. R. Sircar. *Derivatives in Financial Markets with Stochastic Volatility*. Cambridge University Press, September 2000. ISBN 0521791634.
- [Gat04] J. Gatheral. A parsimonious arbitrage-free implied volatility parameterisation with application to the valuation of volatility derivatives. In *TDTF Derivatives Day Amsterdam*, 2004.
- [Gat06] J. Gatheral. *The Volatility Surface: A Practitioner’s Guide*. John Wiley and Sons, 2006. ISBN 0471792519.
- [GJY99] Anja Göing-Jaeschke and Marc Yor. A Survey and some Generalizations of Bessel Processes. Technical report, ETH Zürich, Department of Mathematics, 1999. www.risklab.ch/ftp/papers/GoeingYor.pdf.
- [Hes93] S. L. Heston. A closed-form solution for options with stochastic volatility with applications to bond and currency options. *The Review of Financial Studies*, 6:327–343, 1993.
- [HKL02] P. Hagan, D. Kumar, and A. S. Lesniewski. Managing Smile Risk. *Wilmott*, pages 84–108, September 2002.
- [HL05] P. Henry-Labordère. A General Asymptotic Implied Volatility for Stochastic Volatility Models. Technical report, Société Générale, April 2005. ssrn.com/abstract=698601.
- [HW88] J. Hull and A. White. An Analysis of the Bias in Option Pricing Caused by a Stochastic Volatility. *Advances in Futures and Options Research*, 3:27–61, 1988.
- [HW93] M. Hogan and K. Weintraub. The Lognormal Interest Rate Model and Eurodollar Futures. Discussion paper, Citibank, New York, 1993.
- [Jäc06] P. Jäckel. Hyperbolic local volatility. www.jaeckel.org/HyperbolicLocalVolatility.pdf, November 2006.
- [Kah07] C. Kahl. *Modeling and simulation of stochastic volatility in finance*. PhD thesis, Bergische Universität Wuppertal and ABN AMRO, 2007. Published by www.dissertation.com, www.amazon.com/Modelling-Simulation-Stochastic-Volatility-Finance/dp/1581123833/, ISBN-10: 1581123833.
- [Kaw02] A. Kawai. Analytical and Monte Carlo swaption pricing under the forward swap measure. *Journal of Computational Finance*, 6(1):101–111, 2002. www.maths.unsw.edu.au/statistics/files/preprint-2002-12.pdf.
- [Kaw03] A. Kawai. A new approximate swaption formula in the LIBOR market model: an asymptotic expansion approach. *Applied Mathematical Finance*, 10(1):49–74, March 2003. www.maths.unsw.edu.au/statistics/files/preprint-2002-13.pdf.
- [KJ05] C. Kahl and P. Jäckel. Not-so-complex logarithms in the Heston model. *Wilmott*, September:94–103, September 2005.
- [Klu02] T. Kluge. Pricing derivatives in stochastic volatility models using the finite difference method. Master’s thesis, Technische Universität Chemnitz, September 2002. kluge.in-chemnitz.de/documents/diploma/diploma.pdf.

- [KP99] P. E. Kloeden and E. Platen. *Numerical Solution of Stochastic Differential Equations*. Springer, 1992, 1995, 1999.
- [KT03] N. Kunitomo and A. Takahashi. Applications of the Asymptotic Expansion Approach based on Malliavin-Watanabe Calculus in Financial Problems. CIRJE F-Series CIRJE-F-245, CIRJE, Faculty of Economics, University of Tokyo, November 2003. www.e.u-tokyo.ac.jp/cirje/research/dp/2003/2003cf245.pdf.
- [Lip02] A. Lipton. The vol smile problem. *Risk*, February 2002.
- [MN03] S. Mikhailov and U. Nögel. Heston's Stochastic Volatility Model: Implementation, Calibration, and some Extensions. *Wilmott*, July:74–79, 2003.
- [Osa06] Y. Osajima. The asymptotic expansion formula of implied volatility for dynamic SABR model and FX hybrid model. Technical report, University of Tokyo, Graduate School of Mathematical Sciences, Komaba, Tokyo, Japan, 2006. kyokan.ms.u-tokyo.ac.jp/users/preprint/pdf/2006-29.pdf.
- [Pit03] V. Piterbarg. A Stochastic Volatility Forward Libor Model with a Term Structure of Volatility Smiles. Technical report, Bank of America, 2003. ssrn.com/abstract=472061.
- [Pit07] V. Piterbarg. Markovian projection for volatility calibration. *Risk*, 4, 2007.
- [PTVF92] W. H. Press, S. A. Teukolsky, W. T. Vetterling, and B. P. Flannery. *Numerical Recipes in C*. Cambridge University Press, 1992. www.library.cornell.edu/nr/cbookcpdf.html.
- [Rub83] M. Rubinstein. Displaced diffusion option pricing. *Journal of Finance*, 38:213–217, March 1983.
- [RW03] H. Rasmussen and P. Wilmott. Asymptotic analysis of stochastic volatility models. In *The best of Wilmott : including the latest research from quantitative finance, Review 2003, Vol. 1*, January 2003.
- [Sco87] L. Scott. Option Pricing When the Variance Changes Randomly: Theory, Estimation and An Application. *Journal of Financial and Quantitative Analysis*, 22:419–438, December 1987.
- [SS94] K. Sandmann and D. Sondermann. On the stability of log-normal interest rate models and the pricing of Eurodollar futures. Discussion paper, Dept. of Statistics, Faculty of Economics, SFB 303, Universität Bonn, June 1994. ftp://ftp.wipol.uni-bonn.de/pub/RePEc/bon/bonsfb/bonsfb263.pdf.
- [UO30] G.E. Uhlenbeck and L.S. Ornstein. On the theory of Brownian motion. *Physics Review*, 36:823–841, 1930.
- [Wat87] S. Watanabe. Analysis of Wiener functionals (Malliavin calculus) and its application to heat kernels. *The Annals of Probability*, 15:1–39, 1987.
- [Wig87] J. Wiggins. Option values under stochastic volatility: Theory and empirical estimates. *Journal of Financial Economics*, 19:351–372, 1987.
- [Wil06] P. Wilmott. "Data suggests that for equities and indices $dv = \dots + \alpha v^p dX$ where p is about 1.", 2006. www.wilmott.com/messageview.cfm?catid=4&threadid=41826&FTVAR_MSGDBTABLE=&STARTPAGE=1.